Synergistic Memory Impairment Through the Interaction of Chronic Cerebral Hypoperfusion and Amlyloid Toxicity in a Rat Model

Bo-Ryoung Choi, MA; Sang Rim Lee, BA; Jung-Soo Han, PhD; Sang-Keun Woo, PhD; Kyeong Min Kim, PhD; Dong-Hee Choi, PhD; Kyoung Ja Kwon, PhD; Seol-Heui Han, MD; Chan Young Shin, PhD; Jongmin Lee, MD; Chin-Sang Chung, MD; Seong-Ryong Lee, MD; Hahn Young Kim, MD

Background and Purpose—Vascular pathology and Alzheimer disease (AD) pathology have been shown to coexist in the brains of dementia patients. We investigated how cognitive impairment could be exacerbated in a rat model of combined injury through the interaction of chronic cerebral hypoperfusion and amyloid beta (Aβ) toxicity.

Methods—In Wistar rats, chronic cerebral hypoperfusion was modeled by permanent occlusion of bilateral common carotid arteries (BCCAo). Further, AD pathology was modeled by bilateral intracerebroventricular Aβ (Aβ toxicity) using a nonphysiological Aβ peptide (Aβ 25 to 35). The experimental animals were divided into 4 groups, including sham, single injury (Aβ toxicity or BCCAo), and combined injury (BCCAo-Aβ toxicity) groups (n=7 per group) . Cerebral blood flow and metabolism were measured using small animal positron emission tomography. A Morris water maze task, novel object location and recognition tests, and histological investigation, including neuronal cell death, apoptosis, neuroinflammation, and AD-related pathology, were performed.

Results—Spatial memory impairment was synergistically exacerbated in the BCCAo–Aβ toxicity group as compared to the BCCAo or Aβ toxicity groups ($P<0.05$). Compared to the sham group, neuroinflammation with microglial or astroglial activation was increased both in multiple white matter lesions and the hippocampus in other experimental groups. AD-related pathology was enhanced in the BCCAo–Aβ toxicity group compared to the Aβ toxicity group.

Conclusion—Our experimental results support a clinical hypothesis of the deleterious interaction between chronic cerebral hypoperfusion and Aβ toxicity. Chronic cerebral hypoperfusion-induced perturbation in the equilibrium of AD-related pathology may exacerbate cognitive impairment in a rat model of combined injury. **(*Stroke*. 2011;42:2595-2604.)**

Key Words: Alzheimer disease ■ amyloid beta ■ chronic cerebral hypoperfusion ■ Morris water maze ■ vascular dementia

Alzheimer disease (AD) and vascular dementia are the most common causes of cognitive decline in the aging population.[1] Accumulation of insoluble amyloid beta (Aβ) in the brain has been identified as the major culprit for the cognitive impairment observed in AD patients.[2] Because senile plaques composed of the Aβ peptide have been found in the brains of AD patients,[2] extensive research has focused on the amyloid hypothesis to explain AD pathology.

A hypothesis emphasizing the interaction between AD and vascular pathologies has recently emerged.[3–5] The Nun study and other clinico-pathological studies[6–8] have revealed that patients with AD exhibit concomitant vascular lesions in the brain. Further, epidemiological studies have shown that the major risk factors for AD mostly coincide with those for vascular dementia.[4] The Rotterdam study,[9] a large population-based prospective study, reported an increased prevalence of atherosclerosis in patients either with AD or

Received March 11, 2011; accepted March 31, 2011.

From the Department of Neurology (B.R.C., K.J.K., S.H.H., H.Y.K.), Department of Medicine (D.H.C.), Department of Pharmacology (C.Y.S.), Department of Rehabilitation Medicine (J.L.), Konkuk University School of Medicine, Seoul, Korea; Department of Biological Sciences (B.R.C., S.R.L., J.S.H.), Konkuk University, Center for Geriatric Neuroscience Research, Institute of Biomedical Science and Technology, Seoul, Republic of Korea; Laboratory of Nuclear Medicine Research (S.K.W., K.M.K.), Molecular Imaging Research Center, Korea Institute of Radiological and Medical Sciences (KIRAMS), Seoul, Republic of Korea; Department of Neurology (C.S.C.), Samsung Medical Center, Sungkyunkwan University School of Medicine, Seoul, Republic of Korea; Department of Pharmacology (S.R.L.), Keimyung University School of Medicine and Brain Research Institute, Taegu, Republic of Korea.

The online-only Data Supplement is available at http://stroke.ahajournals.org/cgi/content/full/STROKEAHA.111.620179/DC1.

Correspondence to Hahn Young Kim, MD, Department of Neurology, Konkuk University School of Medicine, Center for Geriatric Neuroscience Research, Institute of Biomedical Science and Technology, 4-12 Hwayang-dong Gwangjin-gu, Seoul, 143-729 Republic of Korea. E-mail hykimmd@gmail.com

Stroke **is available at http://stroke.ahajournals.org** **DOI: 10.1161/STROKEAHA.111.620179**

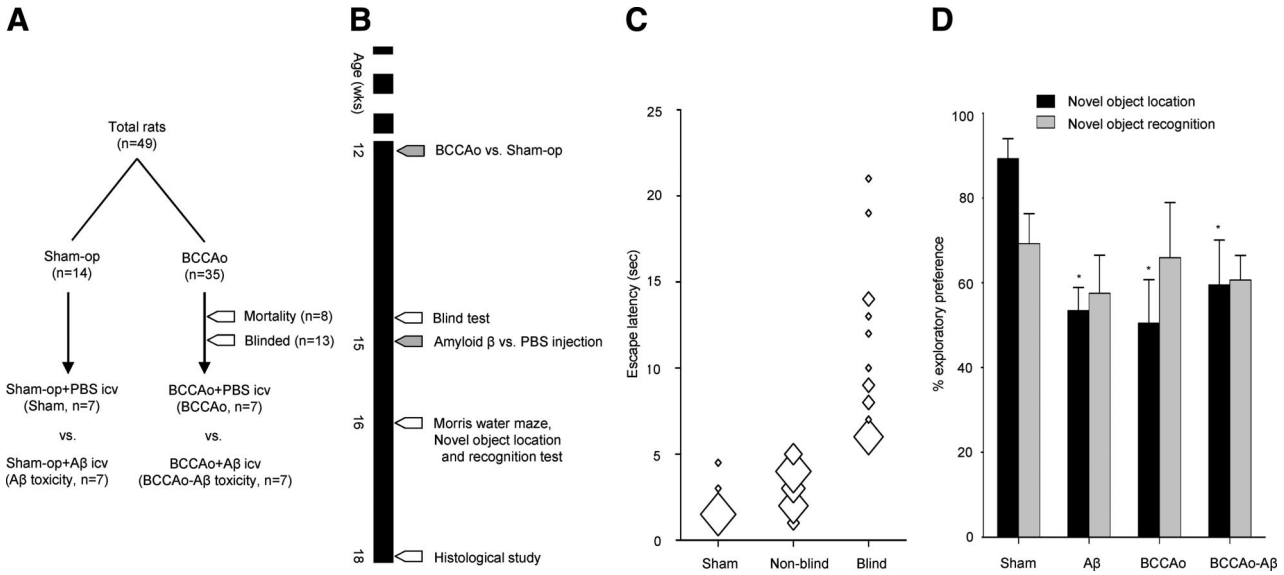

Figure 1. A, Allocation table for each group. Mortality and blindness occurred only in rats with permanent occlusion of bilateral common carotid arteries. **B**, The timeline of the experiment. The rats underwent permanent occlusion of bilateral common carotid arteries or sham operation at 12 weeks. Additional amyloid β or phosphate-buffered saline injection was performed at 15 weeks after screening for blindness. Behavioral tests and histological evaluation were performed at 16 and 18 weeks, respectively. **C**, Escape latency longer than mean plus 3 SD of sham-operated rats was used as an arbitrary cut-off to determine blindness. Sham (n=8), nonblind (n=20), and blind (n=17). **D**, Compared to sham-operated rats, percent exploratory preference in the novel object location test was significantly decreased in other experimental groups ($P<0.05$); n=3 in each group. Aβ, bilateral amyloid β injection; BCCAo, permanent occlusion of bilateral common carotid arteries; BCCAo-Aβ, combined injury of BCCAo and Aβ; icv, intracerebroventricular injection. *$P<0.05$ compared with the sham group on post hoc analysis.

with vascular dementia. In recent imaging studies, vascular lesions such as white matter ischemic changes or lacunar infarction have been suggested as risk factors for cognitive decline in patients with AD.[10]

A converging hypothesis involving chronic cerebral hypoperfusion and AD pathology originally has been suggested in clinical studies.[11–13] Furthermore, the double-hit vascular hypothesis of AD, based on molecular and cellular experimental studies, has been proposed.[14–17] An intact functional neurovascular unit is an active system prerequisite to maintain normal brain function.[15] Entry of peptides in the brain is limited by the blood–brain barrier, unless there is a specific receptor-mediated or carrier-mediated transport, as in case of amino acids.[17–19] The concept of blood–brain barrier dysfunction in a progressive age-dependent vascular-mediated secondary neurodegeneration has been suggested.[16,17]

However, how these 2 distinct vascular and AD pathologies interact has not been clearly established. Recent animal experiments using a rat model with combined injury of lacunar infarction and Aβ toxicity revealed that vascular insults exacerbated AD pathology.[20] Aside from lacunar infarction, we hypothesized that chronic cerebral hypoperfusion may be an exacerbating factor for AD pathology and cognitive impairment. Modeling vascular dementia in animals has been demonstrated by permanent occlusion of the bilateral common carotid arteries in rats.[21–23] Further, intraventricular injection of Aβ has been reported as a method for modeling of AD in rats.[24,25] In the current study, we investigated how cognitive impairment could be synergistically exacerbated in a combined injury model of chronic cerebral hypoperfusion and Aβ toxicity in rats.

Materials and Methods

Experimental Groups

Male Wistar rats were used in these experiments (Charles River, Gapeung, Republic of Korea). All rats resided in the vivarium at Konkuk University for 2 weeks before the beginning of the experiment. The rats were housed at a controlled temperature (22°C±1°C) and humidity (50%±10%) on a 12-hour alternate light–dark cycle. Food and water were provided ad libitum throughout the experiment. All animal experimental procedures were in accordance with the approved guidelines of the Institutional Animal Care and Use Committee of Konkuk University.

The experimental animals were divided into 4 groups using a 2-by-2 table of permanent occlusion of bilateral common carotid arteries (BCCAo) or bilateral Aβ 25 to 35 intracerebroventricular injection (Aβ toxicity), including sham, Aβ toxicity, BCCAo, and BCCAo–Aβ toxicity groups (Figure 1A). Detailed procedures are described in the Supplemental Methods (http://stroke.ahajournals.org). A timeline for surgical procedures for single (Aβ toxicity or permanent occlusion of bilateral common carotid arteries) or combined injury (permanent occlusion of common carotid arteries and Aβ toxicity) and other tests were described (Figure 1B).

Behavioral Test

Water maze task and novel object location and recognition behavior tests were performed to evaluate cognitive impairment. Before the water maze task, a blind test was performed to exclude blinded rats. Detailed procedures are described in the Supplemental Methods.

Cerebral Blood Flow and Metabolism Measurement

Cerebral blood flow and metabolism were measured by ^{18}F-fluorodeoxyglucose positron emission tomography scanner in the acute and chronic phases after permanent occlusion of bilateral common carotid arteries. First 5-minute and between 60- and 80-minute scans of ^{18}F-fluorodeoxyglucose uptake were used as

indicators of cerebral blood flow and metabolism, respectively.[26,27] Detailed procedures are described in the Supplemental Methods.

Histological Investigation

Six weeks after sham operation or permanent occlusion of bilateral common carotid arteries (ie, 3 weeks after Aβ or phosphate-buffered saline injection), thionin staining, terminal deoxynucleotidyl transferase dUTP nick end labeling, and immunohistochemisty, including OX-6, Iba-1, glial fibrillary acidic protein, NeuN, MAP-2, laminin, amyloid β 1 to 42, amyloid precursor protein (APP), and tau-2, were performed. Quantitative analysis was performed when it was needed. Detailed procedures and antibody information are described in the Supplemental Methods.

Statistical Analysis

Parameters for spatial memory, including search error, time latency, and path length, as well as swimming speed, were analyzed by 1-way repeated-measure ANOVA followed by a post hoc Fisher protected least-significant differences test. One-way ANOVA was conducted to compare results of the probe trials, cued behavior, percent exploratory preference, and the quantitative data of the immunohistochemstry (mean$\pm$SE). A value of $P<0.05$ was considered to be statistically significant. Data analyses were performed with the SPSS software version 12.0.

Results

Mortality and Blindness

All procedures for the permanent occlusion of bilateral common carotid arteries were completed within 15 minutes. By the time of Aβ or phosphate-buffered saline injection, the mortality rate was 22.9% (8 of 35) in the permanent occlusion of bilateral common carotid arteries group and 0% (0 of 14) in the sham-operated group (Figure 1A). Before Aβ or phosphate-buffered saline injection, rats with escape latency longer than the blindness cut-off were considered blind and were excluded from further experiments (Figure 1C). The blindness rate among surviving rats was 48.1% (13 of 27) in the permanent occlusion of bilateral common carotid arteries group and 0% (0 of 14) in the sham-operated group (Figure 1A). Fourteen surviving nonblinded rats from each group were equally allocated for an additional Aβ or phosphate-buffered saline injection procedure. No mortality related to the Aβ or phosphate-buffered saline injection procedure developed, and no major neurological deficits impairing motor function, such as forelimb flexion or unilateral circling, were observed in any group. Ultimately, 7 rats per group were used for the behavioral test and 4 per group were used for the histological study.

Cerebral Blood Flow Measurement

After permanent occlusion of bilateral common carotid arteries, the first 5-minute uptake of ^{18}F-fluorodeoxyglucose indicating cerebral blood flow in the cortex was decreased to 96.8% of the baseline at 3 days, 98.3% at 5 weeks, and 74.5% at 8 weeks (Figure 2A). Decreased cerebral blood flow in the cortex was not evident at 3 days and 5 weeks after permanent occlusion of bilateral common carotid arteries; however, decreased pattern was shown at 8 weeks. Between 60- and 80-minute uptake of ^{18}F-fluorodeoxyglucose, indicating cerebral metabolism in the cortex, was decreased to 83.1% of the baseline at 3 days, 80.1% at 5 weeks, and 80.3% at 8 weeks after permanent occlusion of bilateral common carotid arteries (Figure 2B). Compared to the slightly recovered pattern of the metabolism in the striatum and hippocampus, decreased metabolism in the cortex was sustained over the course of 8 weeks.

Behavioral Test

Parameters for spatial memory were significantly different among groups with respect to search error ($P<0.001$), time latency ($P<0.001$), and path length ($P<0.001$; Figure 3A). Swimming speed was not different among groups ($P=0.27$; Figure 3B). Among the 4 groups, the rats with BCCAo–Aβ toxicity showed maximally increased search error, time latency, and path length. On post hoc analysis, the rats with BCCAo exhibited increased search error ($P<0.05$), time latency ($P<0.01$), and path length ($P<0.01$) compared to rats with sham operation or Aβ toxicity (Figure 3A). When Aβ toxicity was added to the permanent occlusion of bilateral common carotid arteries injury (ie, the BCCAo–Aβ toxicity group), there was a synergistic increase in both search error ($P<0.05$) and time latency ($P<0.05$) compared to the BCCAo group. In the first probe trial, the time in the target quadrant was not different among groups ($P=0.22$); however, in the second probe trial, the time in the target quadrant increased up to >40% in sham-operated rats, implicating effective learning and a difference among groups ($P<0.05$). On post hoc analysis, the time spent in the target quadrant significantly decreased in rats with Aβ toxicity ($P<0.05$), BCCAo ($P<0.05$), and BCCAo–Aβ toxicity ($P<0.01$) compared to sham-operated rats (Figure 3C). Cued time latency to reach the visible platform was not different among groups ($P=0.27$; Figure 3D).

On the novel object location test, percent exploratory preference was significantly different among groups ($P<0.05$). On post hoc analysis, percent exploratory preference significantly decreased in rats with Aβ toxicity ($P<0.05$), BCCAo ($P<0.05$), and BCCAo–Aβ toxicity ($P<0.05$) compared to sham-operated rats (Figure 1D). On the novel object recognition test, percent exploratory preference was not different among groups ($P=0.80$; Figure 1D).

Capillary Damages

Laminin staining showed no definite changes of vascular basement membrane in the capillaries or total length of the capillaries in the cortex among experimental groups (Figure 2C).

Apoptosis or Changes in Neuronal Morphology

Thionin staining of the hippocampus demonstrated no significant morphological changes of neurons in the CA1, CA3, and dentate gyrus in any group (Figure 4A). Additional staining including transferase dUTP nick end labeling (Figure 4B), NeuN, and MAP-2 staining (Figure 4C) showed no significant apoptosis or any neuronal morphological changes in the CA1. Further, no definite cell death was observed in the cortex and striatum in any group (data not shown).

Neuroinflammation

As reported in previous studies using rats with permanent occlusion of bilateral common carotid arteries, a microglial

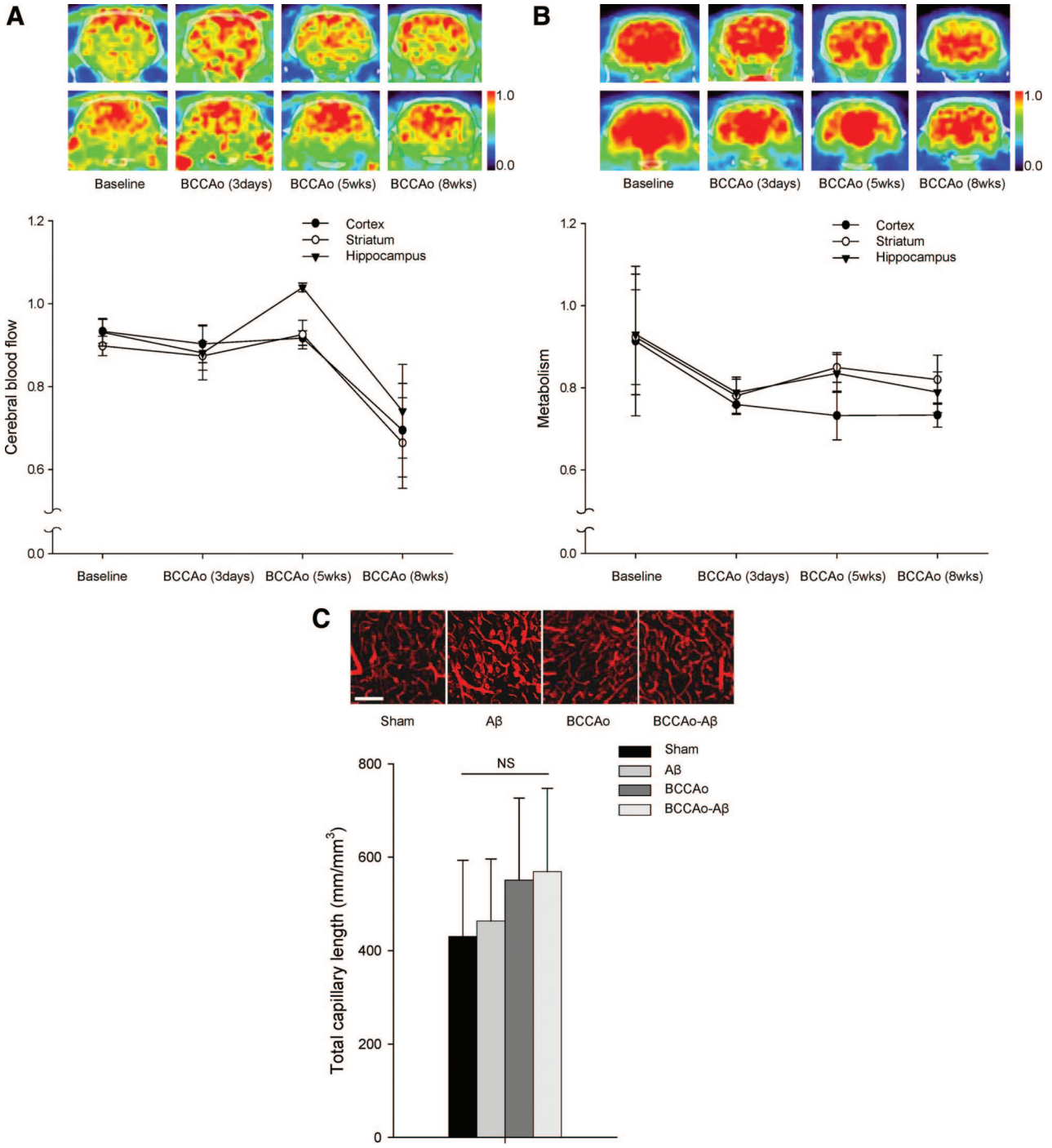

Figure 2. Representative positron emission tomography coronal images superimposed on CT images and temporal profiles of the mean normalized ^{18}F-fluorodeoxyglucose uptake during the first 5 minutes (**A**) and between 60 and 80 minutes (**B**) in the cortex, striatum, and hippocampus; n=3. No morphological changes of capillaries using laminin and no difference of the total capillary length were observed (**C**); n=3 in each group. Aβ, bilateral amyloid β injection; BCCAo, permanent occlusion of bilateral common carotid arteries; BCCAo-Aβ, combined injury of BCCAo and Aβ. Scale bar=100 um.

marker of the neuroinflammation (OX-6) increased in the white matter region, including the corpus callosum and fimbria of the hippocampus, as well as in the internal capsule (Figure 5A). Microglial activation was also induced in rats with Aβ toxicity and BCCAo–Aβ toxicity. Microglial activation in other region, including the cortex, striatum, and hippocampus, was not as prominent as in the white matter region (data not shown). OX-6 staining also can mark peripheral monocytes or macrophages that have entered the brain through a damaged blood–brain barrier. However, OX-6–positive activated microglial cells, displaying a larger amoeboid form with stubby processes, were colocalized with Iba-1, suggestive of the central nervous system origin (lowest column in Figure 5A).

An astroglial marker of the neuroinflammation (glial fibrillary acidic protein) increased in the CA1, CA3, and dentate

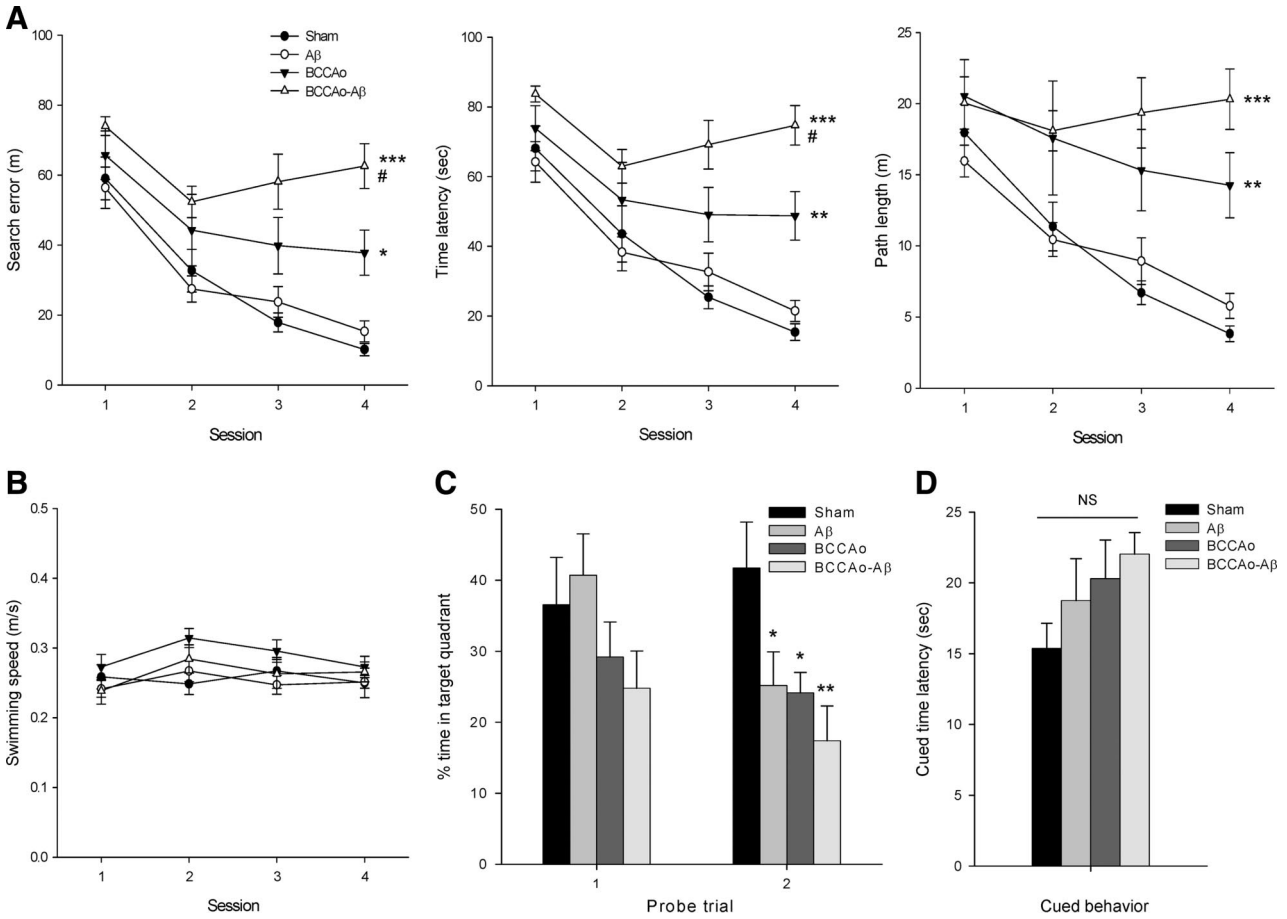

Figure 3. Spatial memory evaluation using several parameters, including search error, time latency, path length (**A**) and swimming speed (**B**). Spatial memory impairment was synergistically exacerbated in the BCCAo-Aβ group, as compared to either the BCCAo or Aβ group. In the second probe trial, the percent of time spent in the target quadrant was increased in sham-operated rats compared to the rats from the other experimental groups ($P<0.05$) (**C**). Time latency in the cued behavior was not different among groups (**D**); n=7 in each group. Aβ, bilateral amyloid β injection; BCCAo, permanent occlusion of bilateral common carotid arteries; BCCAo-Aβ, combined injury of BCCAo and Aβ; NS, not significant. *$P<0.05$, **$P<0.01$, and ***$P<0.001$ compared with the sham group. #$P<0.05$ compared with BCCAo group.

gyrus subfields of the hippocampus in rats with Aβ toxicity, BCCAo, or BCCAo–Aβ toxicity (Figure 5C). Further, astroglial activation also was induced in the white matter lesions, where microglial activation was enhanced (data not shown).

Quantitative analysis revealed that compared to the sham group, neuroinflammation with microglial ($P<0.01$ in the corpus callosum; $P<0.05$ in the fimbra of the hippocampus) or astroglial ($P<0.05$ in the CA1 and CA3; $P<0.01$ in the dentate gyrus) activation was increased both in multiple white matter lesions and the hippocampus in other experimental groups (Figure 5B, D). However, no synergistic increase in neuroinflammation was observed in rats with BCCAo–Aβ toxicity compared to rats with Aβ toxicity or BCCAo.

AD-Related Pathology

AD-related pathology was scarcely observed in the white matter region in any group. Deposition of Aβ in the cortex and striatum was not different among rats with a single or combined injury (data not shown). Both APP and tau-2 pathology were scarcely and randomly observed in the cortex and striatum in sham-operated rats. In rats with BCCAo–Aβ toxicity, APP staining showed enhanced immunoreactivity with sporadic cellular or clustered plaque patterns in the cortical or deep gray matter (Figure 6A) and tau-2 staining with sporadic cellular patterns in the cortical gray matter (Figure 6B) compared to rats with Aβ toxicity. Quantitative analysis revealed that, compared to the sham group, AD-related pathology was increased in other experimental groups ($P<0.01$; Figure 6C). The tau-2 pathology was especially significantly increased in rats with BCCAo–Aβ toxicity compared to rats with a single injury (ie, Aβ toxicity or BCCAo).

Discussion

Spatial Memory Impairment Synergistically Exacerbated by the Combined Injury of Chronic Cerebral Hypoperfusion and Amyloid Toxicity

Chronic cerebral hypoperfusion has been assumed as a pathogenic mechanism in patients with not only vascular dementia but also AD.[4,5] Cognitive impairment has been demonstrated in animals with chronic cerebral hypoperfusion, modeling patients with vascular dementia.[21,28] Results of our experiment were in accordance with previous studies that replicated spatial memory impairment in rats with permanent

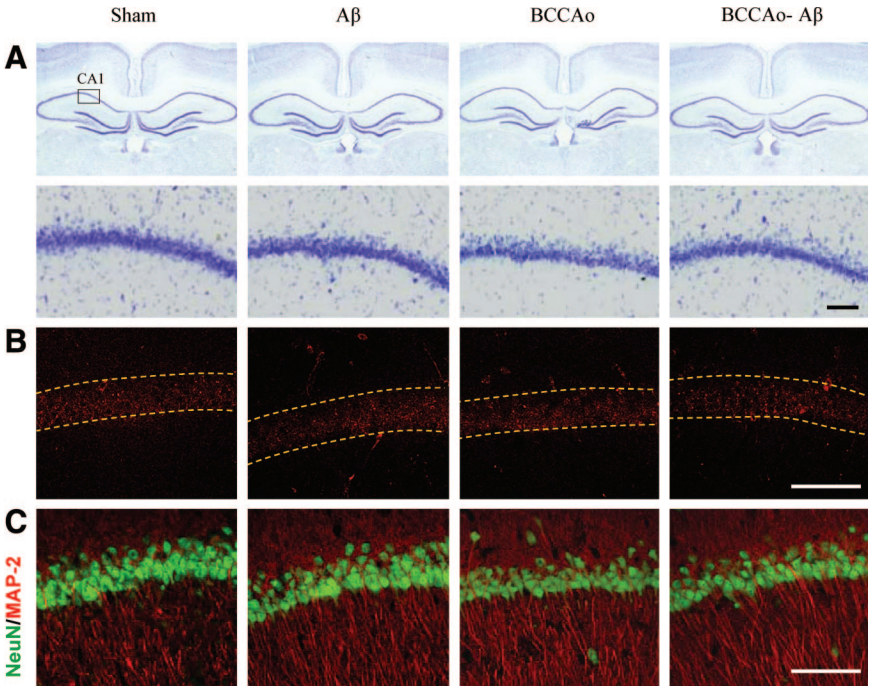

Figure 4. Thionin-stained hippocampus and magnification of CA1 showed no significant neuronal cell death (**A**). Both transferase dUTP nick end labeling (**B**) and NeuN and MAP-2 (**C**) staining showed no significant apoptosis or morphological changes in CA1 neurons. Aβ, bilateral amyloid β injection; BCCAo, permanent occlusion of bilateral common carotid arteries; BCCAo-Aβ, combined injury of BCCAo and Aβ. Scale bar=100 um.

occlusion of bilateral common carotid arteries. With respect to swimming path analysis, the search error, time latency, and path length to find a hidden platform were increased in rats with BCCAo, although the swimming speed was not different among groups. Rats with a visual disturbance were excluded by a blind test before the water maze task and cued time latency dependent on the visual information was not different among rats included in our study. Additionally, other cognitive tests relatively unrelated to the visual ability, such as novel object location and recognition test, also showed some cognitive impairment in rats with BCCAo. Taken together, delays in finding a hidden platform may have occurred because of the spatial memory impairment, rather than being produced by motor or visual dysfunction.

In previous studies, diverse animal models with Aβ toxicity showed cognitive impairment in various behavioral tests.[24,25,29] However, in our experiment, rats with Aβ toxicity did not show any spatial memory impairment through an analysis of the swimming path. According to the post hoc analysis of the swimming path, spatial memory impairment that was initially induced by the permanent occlusion of bilateral common carotid arteries became significantly exacerbated by additional Aβ toxicity in rats with combined injury (BCCAo–Aβ toxicity). In the second probe trial, the time to swim in a target quadrant was >40% in sham-operated rats, demonstrating normal memory consolidation with respect to spatial learning (ie, rats remembering where the hidden platform was). According to the post hoc analysis of the second probe trial, spatial memory was significantly impaired in all 3 injury groups (Aβ toxicity, BCCAo, and BCCAo–Aβ toxicity). Interestingly, this included the Aβ toxicity group in which spatial memory impairment was not initially evident in the swimming path analysis compared to sham-operated rats. In general, a trend for severe spatial memory impairment in rats with combined injury was demonstrated in probe trials.

Another behavioral test including novel object location and recognition test was performed to confirm memory impairment in our animal models.[16,30,31] The novel object location test, indicating more hippocampal specific memory, showed significant difference among groups.[30] Compared to sham-operated rats, other experimental groups showed significant memory impairment, although a synergistic pattern was not observed in rats with BCCAo–Aβ toxicity. In contrast, the novel object recognition test, indicating perirhinal cortex-mediated memory consolidation,[16,31] showed no significant difference among groups.

Aβ toxicity in our model may not be enough to induce full-blown cognitive impairment, because rats with Aβ toxicity showed memory impairment only in the analysis of probe trials and the novel object location test. Too short time interval between Aβ injection and behavioral tests or too low concentration of used Aβ may have been the reason why the rats with Aβ toxicity failed to show definite cognitive impairment. However, our Aβ toxicity model with subtle cognitive impairment may be more appropriate to test the hypothesis of synergistic exacerbation of chronic cerebral hypoperfusion and Aβ toxicity than already full-blown AD models. Regarding synergism, when minimal Aβ toxicity was combined by the permanent occlusion of bilateral common carotid arteries, the BCCAo–Aβ toxicity group showed statistically significant synergism of memory impairment beyond the baseline memory impairment initially induced by the permanent occlusion of bilateral common carotid arteries. Similarly, AD-related pathology that was initially minimal in rats with Aβ toxicity was also enhanced when Aβ toxicity was combined with permanent occlusion of bilateral common carotid arteries. Therefore, although Aβ toxicity itself in our model may not have been

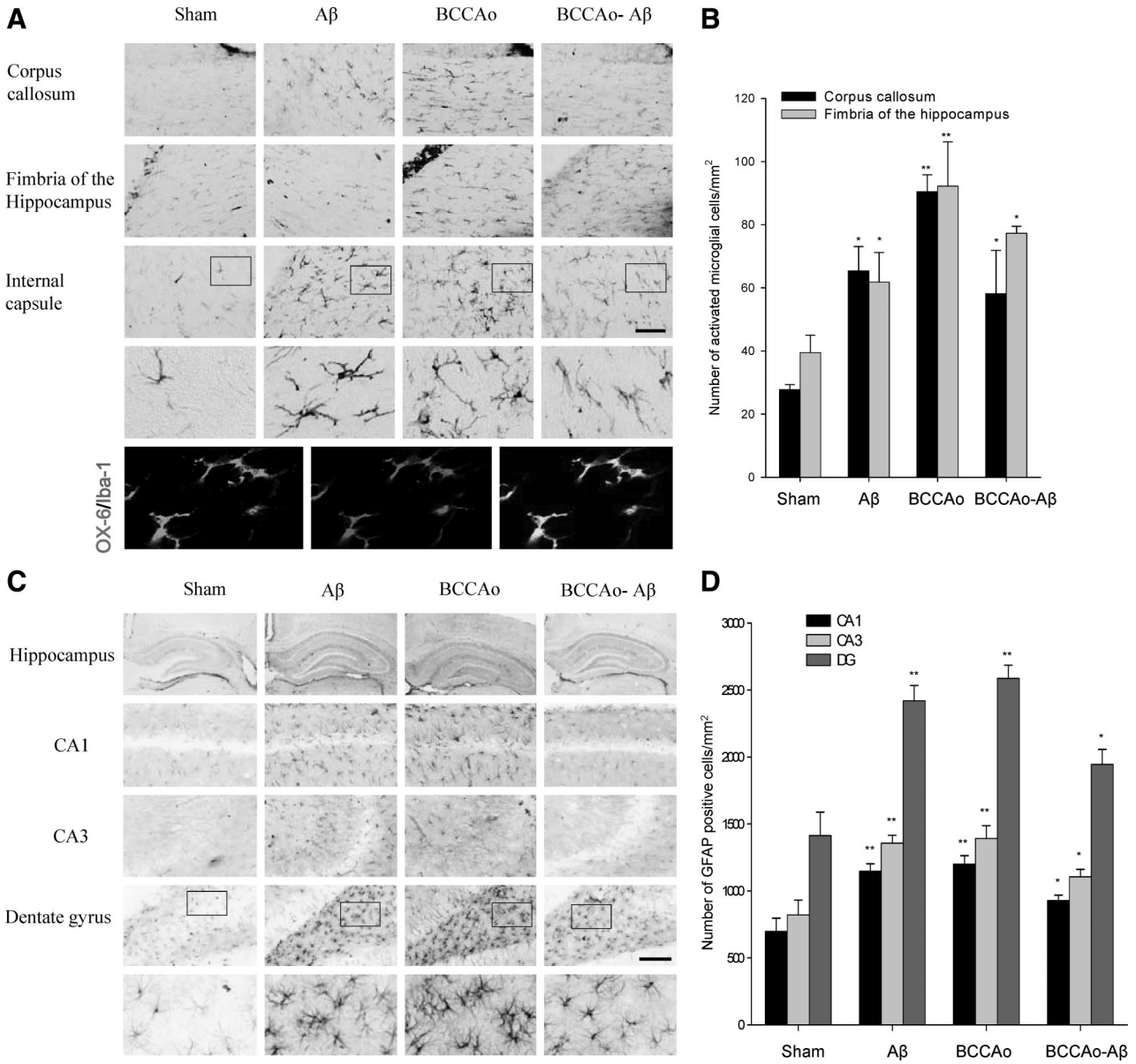

Figure 5. Neuroinflammation measured by microglial and astroglial activation. **A**, OX-6 immunoreactivity in the corpus callosum, fimbria of the hippocampus, and internal capsule, with magnification of the insets. OX-6–positive activated microglial cells were colocalized with Iba-1 (lowest column of **A**). **B**, Quantitative analysis by counting active microglial cells under high magnification. **C**, Glial fibrillary acidic protein immunoreactivity in the hippocampus and magnified subfields of the CA1, CA3, and the dentate gyrus (DG), with magnification of the insets. **D**, Quantitative analysis by counting astroglial cells under high magnification; n=4 in each group. Aβ, bilateral amyloid β injection; BCCAo, permanent occlusion of bilateral common carotid arteries; BCCAo-Aβ, combined injury of BCCAo and Aβ. Scale bar=200 um. *$P<0.05$ and **$P<0.01$ compared with the sham group.

enough to induce spatial memory impairment independently, subclinical Aβ toxicity could have played a synergistic role when it was combined with critically impaired cerebral hypoperfusion.

Taken together, results of behavioral tests and histological investigations in our experiment support the clinical hypothesis that chronic cerebral hypoperfusion and AD pathology could interact in a synergistically exacerbating manner.

Mechanism of Combined Injury From Chronic Cerebral Hypoperfusion and Amyloid Toxicity

A converging hypothesis has emerged to explain the interaction between vascular and AD pathologies.[3–5] However, how these pathologies interact with each other has not been clearly studied. In the current study, we investigated neuronal cell death in the hippocampus to explain spatial memory impairment. Cell death and diffuse atrophy of the hippocampus with behavioral impairment have been reported in a rat model of transient global ischemia or chronic cerebral hypoperfusion.[21,32] On the contrary, no definite morphological change in neurons or atrophy of the hippocampus was observed in any of our experimental groups. Our results suggested that a neuronal toxic effect from the permanent occlusion of bilateral common carotid arteries, Aβ toxicity, or even a combined injury was not strong enough to induce neuronal cell death in the hippocampus.

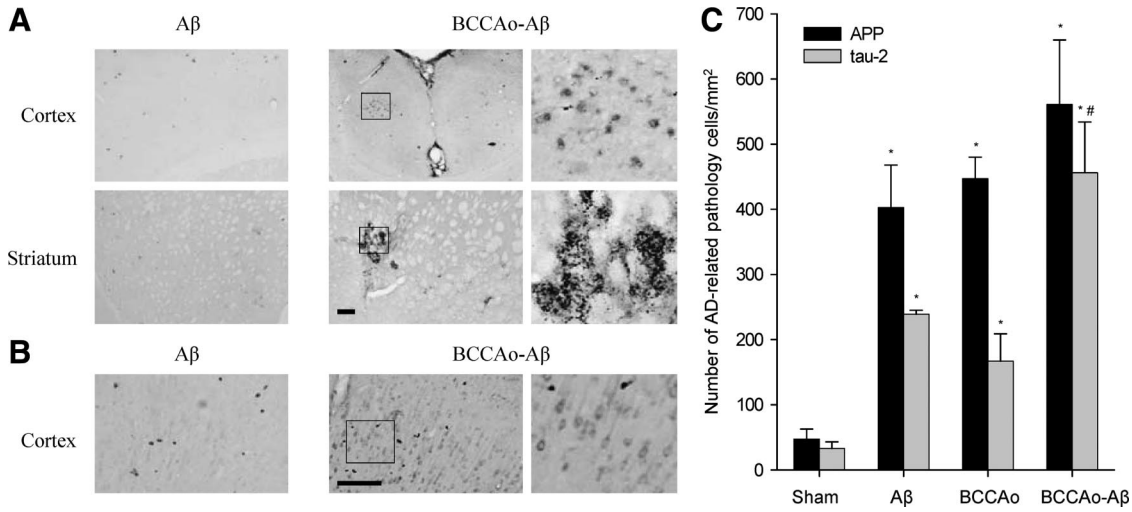

Figure 6. Alzheimer disease-related pathology and magnification of the insets. **A**, Amyloid precursor protein (APP) immunoreactivity was enhanced in the cortex or striatum and magnification of neuronal or plaque form developed in rats with BCCAo-Aβ toxicity compared to those with Aβ toxicity. **B**, The tau-2 immunoreactivity was enhanced in the cortex and magnification of neuronal form occurred in rats with BCCAo–Aβ toxicity compared to those with Aβ toxicity. **C**, Compared to sham-operated rats, quantitative analysis of both APP and tau-2 showed increased immunoreactivity in other experimental groups; n=3 in each group. BCCAo, permanent occlusion of bilateral common carotid arteries; BCCAo-Aβ, combined injury of BCCAo and Aβ. Scale bar=200 um. *$P<0.01$ compared with the sham group. #$P<0.01$ compared with Aβ toxicity or BCCAo group.

Second, we hypothesized that the combined injury of the permanent occlusion of bilateral common carotid arteries and Aβ toxicity may exacerbate neuroinflammation. Neuroinflammation or demyelination with neuroinflammation has been suggested as a key pathological mechanisms of chronic cerebral hypoperfusion.[21–23,33] Further, microglial or astroglial activation in the hippocampus has been reported in animal models of chronic cerebral hypoperfusion or Aβ toxicity.[20,21] A rat model with a combined injury of lacunar infarction and Aβ toxicity showed increased neuroinflammation in the hippocampus.[20] In our experiment, neuroinflammation was increased by the permanent occlusion of bilateral common carotid arteries and Aβ toxicity, as compared to that in sham-operated rats; however, an additional synergistic exacerbating effect was not definite in the combined injury group. Neuroinflammation could not fully explain the synergistic exacerbation that was observed in the spatial memory test in the combined injury group.

Third, we investigated AD-related pathology, including Aβ, APP, and tau. Increased APP deposition has been demonstrated not only in animal models of AD but also in acute or chronic ischemic lesions.[33–35] In addition, APP deposition in the cortex and hippocampus in an ischemic rat model and alteration of Aβ metabolism by chronic cerebral hypoperfusion have been suggested.[36,37] Chronic cerebral hypoperfusion has been shown to accelerate Aβ deposition in an APP transgenic mouse model with chronic stenosis of the bilateral carotid arteries.[38] Furthermore, Aβ deposition in a transgenic mouse model of cerebral amyloid angiopathy has been demonstrated to impair cerebral blood flow regulation.[39] Chronic cerebral hypoperfusion and Aβ toxicity may interact with each other in a deleterious way, rather than a 1-sided cause-and-effect relationship. In our experiment, deposition of Aβ itself in the cortex, striatum, or hippocampus was not different among rats with a single or combined injury. Further, both APP and tau pathology were scarcely and randomly observed in both the cortex and striatum of sham-operated rats. However, APP and tau pathology were enhanced in rats with BCCAo–Aβ toxicity compared to rats with Aβ toxicity. Patterns of APP staining were shown to be sporadic neuronal or conglomerated plaque forms. Therefore, chronic cerebral hypoperfusion may play a key role in triggering Aβ toxicity.

The importance of cerebral blood flow in AD has been well-documented in clinical studies.[11,12] A clinical hypothesis has suggested that regional cerebral hypoperfusion is one of the earliest clinical manifestations in patients with AD.[12] It has been shown that amyloid is in dynamic equilibrium in terms of clearance and kinetics between the brain and blood compartments.[15] In a previous study, mutant Aβ peptides showed reduced clearance from the brain because of lack of affinity for the Aβ peptide carrier, which eliminates Aβ from the cerebrospinal fluid and brain into the vascular circulation.[17] It also has been suggested that perturbation in the equilibrium of amyloid deposition between brain parenchymal and vascular compartments may induce pathological changes.[15,40,41] Further, permanent occlusion of bilateral common carotid arteries-induced suboptimal cerebral perfusion may generate ultrastructural damage of the cerebral capillary walls.[13] In our experiment, this capillary damage may have had some effect on the normal clearance of AD-related pathology. However, no definite morphological changes of the vascular basement membranes in the capillaries were observed. Instead, our serial positron emission tomography study showed decreased cerebral blood flow and metabolism in the various areas of the cerebral hemispheres, especially in the cortex. Although vascular injury in our chronic cerebral hypoperfusion model may not have been enough to induce strong structural capillary damages as in acute ischemic models, functional impairment in the cerebral blood flow and

metabolism may be the main pathogenic mechanisms in our chronic cerebral hypoperfusion model.

In addition, chronic cerebral hypoperfusion has been reported to disturb endogenous AD-related pathology, including APP.[35,37,38] In our experiment, exogenous Aβ in the Aβ toxicity group may not have been enough to induce AD-related pathology and was likely cleared by normal cerebral perfusion. Thus, memory impairment and AD-related pathology may be minimal in this Aβ toxicity group. However, when Aβ toxicity was combined with the permanent occlusion of bilateral common carotid arteries, AD-related pathology was exacerbated. The vascular clearance mechanism may be disrupted in rats with permanent occlusion of bilateral common carotid arteries because of downregulation of low-density lipoprotein receptor-related protein 1, the key Aβ clearance receptor, which has been recently shown to be reduced in AD cerebral vessels via hypoxia-mediated overexpression of vascular specific genes.[42] Further study focused on the Aβ clearance receptor in this rat model of combined injury is needed.

Limitations of Aβ 25 to 35

Aβ 25 to 35 used in our experiment may not have contained the Aβ sequences that play a critical role in both transport and interactions with Aβ putative receptors.[17] The Aβ brain extract produced in vivo showed particular properties that are essential for disseminating AD pathology.[43] Concentration of Aβ 25 to 35 in our experiment was significantly higher than observed levels of endogenous Aβ in patients with AD.[14] Therefore, further study using different confirmations of Aβ peptide (Aβ 1 to 40 or Aβ 1 to 42) with the concentration relevant to clinical AD pathogenesis is needed, because artificial Aβ 25 to 35 may not have the same pathological activity as the endogenous Aβ proteins found in AD patients.

Conclusion

In summary, chronic cerebral hypoperfusion-induced perturbation in the equilibrium of AD-related pathology may exacerbate cognitive impairment in a rat model of combined injury. Thus, maintaining optimal cerebral perfusion may be crucial to prevent further cognitive impairment in patients with AD.

Acknowledgments

The authors thank Kwang Sun Woo for his technical assistance.

Sources of Funding

This work was supported by the Korea Research Foundation Grant funded by the Korean Government (KRF-2008-331-E00298).

Disclosure

None.

References

1. Fratiglioni L, De Ronchi D, Agüero-Torres H. Worldwide prevalence and incidence of dementia. *Drugs Aging*. 1999;15:365–375.
2. Masters CL, Simms G, Weinman NA, Multhaup G, McDonald BL, Beyreuther K. Amyloid plaque core protein in Alzheimer disease and Down syndrome. *Proc Natl Acad Sci U S A*. 1985;82:4245–4249.
3. Casserly I, Topol E. Convergence of atherosclerosis and Alzheimer's disease: inflammation, cholesterol, and misfolded proteins. *Lancet*. 2004; 363:1139–1146.
4. de la Torre JC. Is Alzheimer's disease a neurodegenerative or a vascular disorder? Data, dogma, and dialectics. *Lancet Neurol*. 2004;3:184–190.
5. Skoog I. Vascular aspects in Alzheimer's disease. *J Neural Transm Suppl*. 2000;59:37–43.
6. Jellinger KA. Alzheimer disease and cerebrovascular pathology: an update. *J Neural Transm*. 2002;109:813–836.
7. Lim A, Tsuang D, Kukull W, Nochlin D, Leverenz J, McCormick W, et al. Clinico-neuropathological correlation of Alzheimer's disease in a community-based case series. *J Am Geriatr Soc*. 1999;47:564–569.
8. Snowdon DA, Greiner LH, Mortimer JA, Riley KP, Greiner PA, Markesbery WR. Brain infarction and the clinical expression of Alzheimer disease. The Nun Study. *JAMA*. 1997;277:813–817.
9. Hofman A, Ott A, Breteler MM, Bots ML, Slooter AJ, van Harskamp F, et al. Atherosclerosis, apolipoprotein E, and prevalence of dementia and Alzheimer's disease in the Rotterdam Study. *Lancet*. 1997;349:151–154.
10. Yoshita M, Fletcher E, Harvey D, Ortega M, Martinez O, Mungas DM, et al. Extent and distribution of white matter hyperintensities in normal aging, MCI, and AD. *Neurology*. 2006;67:2192–2198.
11. Ruitenberg A, den Heijer T, Bakker SL, van Swieten JC, Koudstaal PJ, Hofman A, et al. Cerebral hypoperfusion and clinical onset of dementia: the Rotterdam Study. *Ann Neurol*. 2005;57:789–794.
12. de la Torre JC. Critically attained threshold of cerebral hypoperfusion: the CATCH hypothesis of Alzheimer's pathogenesis. *Neurobiol Aging*. 2000; 21:331–342.
13. Farkas E, De Vos RA, Jansen Steur EN, Luiten PG. Are Alzheimer's disease, hypertension, and cerebrocapillary damage related? *Neurobiol Aging*. 2000;21:235–243.
14. Fagan AM, Younkin LH, Morris JC, Fryer JD, Cole TG, Younkin SG, et al. Differences in the Abeta40/Abeta42 ratio associated with cerebrospinal fluid lipoproteins as a function of apolipoprotein E genotype. *Ann Neurol*. 2000;48:201–210.
15. Zlokovic BV. Neurovascular mechanisms of Alzheimer's neurodegeneration. *Trends Neurosci*. 2005;28:202–208.
16. Bell RD, Winkler EA, Sagare AP, Singh I, LaRue B, Deane R, et al. Pericytes control key neurovascular functions and neuronal phenotype in the adult brain and during brain aging. *Neuron*. 2010;68:409–427.
17. Monro OR, Mackic JB, Yamada S, Segal MB, Ghiso J, Maurer C, et al. Substitution at codon 22 reduces clearance of Alzheimer's amyloid-beta peptide from the cerebrospinal fluid and prevents its transport from the central nervous system into blood. *Neurobiol Aging*. 2002;23:405–412.
18. Zloković BV, Segal MB, Begley DJ, Davson H, Rakić L. Permeability of the blood-cerebrospinal fluid and blood-brain barriers to thyrotropin-releasing hormone. *Brain Res*. 1985;358:191–199.
19. Segal MB, Preston JE, Collis CS, Zlokovic BV. Kinetics and Na independence of amino acid uptake by blood side of perfused sheep choroid plexus. *Am J Physiol*. 1990;258:F1288–F1294.
20. Whitehead SN, Hachinski VC, Cechetto DF. Interaction between a rat model of cerebral ischemia and beta-amyloid toxicity: inflammatory responses. *Stroke*. 2005;36:107–112.
21. Liu J, Jin DZ, Xiao L, Zhu XZ. Paeoniflorin attenuates chronic cerebral hypoperfusion-induced learning dysfunction and brain damage in rats. *Brain Res*. 2006;1089:162–170.
22. Farkas E, Donka G, de Vos RA, Mihály A, Bari F, Luiten PG. Experimental cerebral hypoperfusion induces white matter injury and microglial activation in the rat brain. *Acta Neuropathol*. 2004;108:57–64.
23. Lee HJ, Kang JS, Kim YI. Citicoline protects against cognitive impairment in a rat model of chronic cerebral hypoperfusion. *J Clin Neurol*. 2009;5:33–38.
24. Whitehead SN, Cheng G, Hachinski VC, Cechetto DF. Progressive increase in infarct size, neuroinflammation, and cognitive deficits in the presence of high levels of amyloid. *Stroke*. 2007;38:3245–3250.
25. Prediger RD, Franco JL, Pandolfo P, Medeiros R, Duarte FS, Di Giunta G, et al. Differential susceptibility following beta-amyloid peptide-(1–40) administration in C57BL/6 and Swiss albino mice: Evidence for a dissociation between cognitive deficits and the glutathione system response. *Behav Brain Res*. 2007;177:205–213.
26. Mullani NA, Herbst RS, O'Neil RG, Gould KL, Barron BJ, Abbruzzese JL. Tumor blood flow measured by PET dynamic imaging of first-pass ^{18}F-FDG uptake: a comparison with ^{15}O-labeled water-measured blood flow. *J Nucl Med*. 2008;49:517–523.

27. Nishio K, Ihara M, Yamasaki N, Kalaria RN, Maki T, Fujita Y, et al. A mouse model characterizing features of vascular dementia with hippocampal atrophy. *Stroke*. 2010;41:1278–1284.
28. Shibata M, Yamasaki N, Miyakawa T, Kalaria RN, Fujita Y, Ohtani R, et al. Selective impairment of working memory in a mouse model of chronic cerebral hypoperfusion. *Stroke*. 2007;38:2826–2832.
29. Sipos E, Kurunczi A, Kasza A, Horváth J, Felszeghy K, Laroche S, et al. Beta-amyloid pathology in the entorhinal cortex of rats induces memory deficits: implications for Alzheimer's disease. *Neuroscience*. 2007;147:28–36.
30. Lee JS, Im DS, An YS, Hong JM, Gwag BJ, Joo IS. Chronic cerebral hypoperfusion in a mouse model of Alzheimer's disease: an additional contributing factor of cognitive impairment. *Neurosci Lett*. 2011;489:84–88.
31. Winters BD, Bussey TJ. Transient inactivation of perirhinal cortex disrupts encoding, retrieval, and consolidation of object recognition memory. *J Neurosci*. 2005;25:52–61.
32. Langdon KD, Granter-Button S, Corbett D. Persistent behavioral impairments and neuroinflammation following global ischemia in the rat. *Eur J Neurosci*. 2008;28:2310–2318.
33. Wakita H, Tomimoto H, Akiguchi I, Matsuo A, Lin JX, Ihara M, et al. Axonal damage and demyelination in the white matter after chronic cerebral hypoperfusion in the rat. *Brain Res*. 2002;924:63–70.
34. Tomimoto H, Wakita H, Akiguchi I, Nakamura S, Kimura J. Temporal profiles of accumulation of amyloid beta/A4 protein precursor in the gerbil after graded ischemic stress. *J Cereb Blood Flow Metab*. 1994;14:565–573.
35. Kalaria RN, Bhatti SU, Lust WD, Perry G. The amyloid precursor protein in ischemic brain injury and chronic hypoperfusion. *Ann N Y Acad Sci*. 1993;695:190–193.
36. Kalaria RN, Bhatti SU, Palatinsky EA, Pennington DH, Shelton ER, Chan HW, et al. Accumulation of the beta amyloid precursor protein at sites of ischemic injury in rat brain. *Neuroreport*. 1993;4:211–214.
37. Bennett SA, Pappas BA, Stevens WD, Davidson CM, Fortin T, Chen J. Cleavage of amyloid precursor protein elicited by chronic cerebral hypoperfusion. *Neurobiol Aging*. 2000;21:207–214.
38. Kitaguchi H, Tomimoto H, Ihara M, Shibata M, Uemura K, Kalaria RN, et al. Chronic cerebral hypoperfusion accelerates amyloid beta deposition in APPSwInd transgenic mice. *Brain Res*. 2009;1294:202–210.
39. Shin HK, Jones PB, Garcia-Alloza M, Borrelli L, Greenberg SM, Bacskai BJ, et al. Age-dependent cerebrovascular dysfunction in a transgenic mouse model of cerebral amyloid angiopathy. *Brain*. 2007;130:2310–2319.
40. Bell RD, Zlokovic BV. Neurovascular mechanisms and blood-brain barrier disorder in Alzheimer's disease. *Acta Neuropathol*. 2009;118:103–113.
41. Deane R, Wu Z, Zlokovic BV. RAGE (yin) versus LRP (yang) balance regulates alzheimer amyloid beta-peptide clearance through transport across the blood-brain barrier. *Stroke*. 2004;35:2628–2631.
42. Bell RD, Deane R, Chow N, Long X, Sagare A, Singh I, et al. SRF and myocardin regulate LRP-mediated amyloid-beta clearance in brain vascular cells. *Nat Cell Biol*. 2009;11:143–153.
43. Eisele YS, Obermüller U, Heilbronner G, Baumann F, Kaeser SA, Wolburg H, et al. Peripherally applied Abeta-containing inoculates induce cerebral beta-amyloidosis. *Science*. 2010;330:980–982.

Synergistic Memory Impairment Through the Interaction of Chronic Cerebral Hypoperfusion and Amlyloid Toxicity in a Rat Model

Bo-Ryoung Choi, Sang Rim Lee, Jung-Soo Han, Sang-Keun Woo, Kyeong Min Kim, Dong-Hee Choi, Kyoung Ja Kwon, Seol-Heui Han, Chan Young Shin, Jongmin Lee, Chin-Sang Chung, Seong-Ryong Lee and Hahn Young Kim

Stroke. 2011;42:2595-2604; originally published online July 7, 2011;
doi: 10.1161/STROKEAHA.111.620179
Stroke is published by the American Heart Association, 7272 Greenville Avenue, Dallas, TX 75231

Print ISSN: 0039-2499. Online ISSN: 1524-4628

SUPPLEMENT MATERIAL

Synergistic memory impairment through the interaction of chronic cerebral hypoperfusion and amlyloid toxicity in a rat model

Supplemental Methods

Surgical procedures

Chronic cerebral hypoperfusion in the rat (12 weeks old) was modeled by BCCAo. Rats were anesthetized with a 5% isoflurane/oxygen mixture and maintained on 3% isoflurane/oxygen during the surgery. Through a midline incision, the bilateral common carotid arteries were carefully exposed and permanently double ligated with silk sutures. With exception to the BCCAo, the same surgical procedures were performed in sham-operated rats. Rectal temperature was maintained between 37±0.5℃ with a heating pad during the surgery.

Alzheimer's disease pathology was modeled by Aβ toxicity. Three weeks after BCCAo or sham operation, the rats were anesthetized by intraperitoneal injection of a ketamine/xylazine mixture and fixed onto a stereotactic frame (Kopf Instruments, Tujunga, CA, USA). Subsequently, an incisor bar was set at 3.3 mm below the ear bars. After shaving, a surgical area was disinfected with iodine and 70 % ethyl alcohol. Burr holes were then drilled with a diameter of 0.8 mm at the coordinates of anteroposterior -0.8 mm and mediolateral ±1.5 mm from the bregma. Amyloid beta 25-35 (Bachem, Torrance, California) or autoclaved 0.01M phosphate-buffered saline (PBS) were bilaterally injected into the lateral ventricles at a depth of 4 mm. Amyloid beta 25-35 was then prepared at a concentration of 50 nM in 5 ul of saline and bilaterally injected with the velocity of 0.5ul/min. The injecting needle was slowly removed after completion of the injection to prevent overflow regurgitation.

Blind test

Prior to the water maze task, a blind test was performed using a modified method as previously described.[1] Rats were placed in a 90 cm x 45 cm x 32 cm (height) sized box separated by a wall with an open path in the middle (18 cm x 32 cm). The floor of one space was gridded with electrodes and that of another space was flat. After free exploration of the space for 5min, rats were put into the grid space and given a foot shock with 3 mA for 1 sec. Under daylight, rats with normal vision could escape to a safe space through the open path immediately after the shock, while blinded rats were unable to find the path and turned around repeatedly in the grid space. Escape latency longer than the mean plus three standard deviations of sham-operated rats was used as an arbitrary cutoff to determine blindness.

Water maze task

Rats were evaluated in a Morris water maze. The maze was a round tank, 1.83 m in diameter and 0.58 m deep, filled to a depth of 35.5 cm with tepid (26±1℃) water made opaque by the addition of white paint. A moveable circular platform 12 cm in diameter was located 2 cm below the surface of the water. The maze was surrounded by white curtains on which black visual stimuli of various shapes and sizes were placed. A camera was located above the center of the maze which relayed images to a videocassette recorder and an HVS Image Analysis Computer System (Hampton, United Kingdom).

Four weeks after sham operation or BCCAo (one week after Aβ or PBS injection), a Morris water maze task was performed to evaluate spatial memory (n=7 per each group). Four consecutive sessions, each consisting of five trials for two days (alternating two or three trials per day), was conducted on eight consecutive days. The hidden platform was constantly located in the southeast quadrant of the pool. Rats were gently submerged in the water, facing the inside wall of the tank. Every trial started at different points, alternating among four quadrants.

Rats were gently handled for 10 min daily for 7 days before the test. In the maze, rats were allowed to swim for a maximum of 90 sec. Further, they were allowed to remain on the platform for 30 sec at the end of each trial. Performance accuracy was evaluated by the analysis of the search error, time latency, and path length data of all trials. Measurement of the search error was based on a computation of the average distance from the platform during the trial. The distance between rat and the platform was sampled 10 times/sec during each trial and these distances were averaged in 1-sec bins. Cumulative search error is the sum of these 1-sec averages of the proximity measure corrected for the specific platform location and start location by subtracting the proximity score that would be produced by a perfect performance in the trial. A probe trial was conducted 1 min after every 10th training trial. The entire training procedure included two probe trials for each rat, during which the rats swam with the platform retracted to the bottom of the pool for 30 sec. After recording the swimming path, the platform was raised to its normal position for completion of the trial. Swimming time spent in the target quadrant of the retracted platform was used as a parameter for the retention of spatial memory. One week after the completion of the Morris water maze task with a hidden platform, all rats were assessed for cued behavior with a visible platform raised above the surface of the water. The location of the visible platform varied from trial to trial in a single session of six training trials.

Novel object location and recognition behavior test

Four weeks after sham operation or BCCAo (one week after Aβ or PBS injection), a novel object location and recognition behavior test was performed (n=3 per each group). The test was carried out by modification of the method described in a previous study.[2, 3] The rats were placed in a 40 cm x 40 cm x 40 cm (height) sized box and allowed to equilibrate to the testing area 10 minutes per day for 3 days. After 24 hours two objects were placed in the testing area and then the rat was allowed to explore the two objects in the testing area for 5 minutes before being returned to cage. After a 3 hour-interval one of the objects was either re-located or replaced with a new object and the rats were allowed to explore the testing area once again for 2 minutes. Exploring novel object was defined if the center of the rat's head was oriented within 45° of the object and within 4 cm of it. Climbing over or sitting on an object was not included A video camera was positioned over the arena and exploratory behaviors were videotaped for later analysis. Exploratory time spent for novel objects was recorded and percent exploratory preference was computed as [time in novel/(time in novel + time in old object)] in a blind manner.

Motor function

Major neurological deficits that could physically limit swimming ability such as forelimb flexion or unilateral circling were evaluated prior to every trial. Further, swimming speed was monitored during every trial.

Cerebral blood flow measurement

Cerebral blood flow was measured by ^{18}F-fluorodeoxyglucose (^{18}F-FDG) positron emission tomography (PET) scanner, consisting of a 16.1 cm ring diameter with a lutetium oxyorthosilicate crystal, providing a 10 cm transaxial field of view and a 12.7 cm axial field of view, with spatial resolution of <1.8 mm full-width half-maximum at the center and 9.3 % sensitivity within an energy window of 250 – 625 keV (Inveon^{TM}, Siemens Preclinical Solutions, Knoxville, TN, USA). The PET studies were performed 3 days, 5 weeks and 8 weeks after BCCAo surgery (n=3). The rats were anesthetized with 2% isoflurane/oxygen and 37 MBq/0.2 ml (1mCi) of ^{18}F-FDG was intravenously injected through the tail vein. Dynamic acquisition was performed in three-dimensional mode, and the acquired emission data was reconstructed to temporally framed sinograms using Fourier rebinning and the ordered subsets expectation maximization algorithm with 4 iterations. Corrections for dead time, random, scatter, decay, and normalization were performed. First 5 minutes and between 60 and 80 minutes scans of ^{18}F-FDG uptake were used as an indicator of cerebral blood flow and metabolism, respectively, which was suggested in previous studies. [4, 5] The volumes of interest (VOIs) in the standard uptake value images were drawn and calculated on the cortex, striatum, hippocampus and cerebellum areas and counts under the three VOIs (cortex, striatum and hippocampus) were normalized to an average count of the cerebellum as a reference. Representative PET coronal images were superimposed on the CT images.

Brain preparation

Six weeks after sham operation or BCCAo (three weeks after Aβ or PBS injection), rats were intracardially perfused with 0.01M PBS and subsequently with 4% paraformaldehyde (PFA) under deep anesthesia (n=4 per each group). The brain was then removed and post-fixed in 4% PFA for 2 days, cryoprotected in PBS containing 30% sucrose for 48 hours, frozen on powdered dry ice, and sectioned using a microtome.

Thionin and terminal deoxynucleotidyl transferase biotin-dUTP nick end labeling (TUNEL) staining

Perfused brain tissues sectioned on a microtome in a 40um coronal plane were stored in 4℃ PBS. The sections for thionin staining were mounted onto resin coated slide glass, and then dried for 10 days. Sections were hydrated through a descending concentration of ethanol and subsequently dipped twice in distilled water. Sections were stained in thionin solution for a few minutes and washed in distilled water and ethanol, and then dehydrated through ascending concentrations of ethanol. Sections were then defatted in xylene and cover-slipped with permount reagent.

TUNEL staining was performed using commercial kit (In Situ Cell Death Detection Kit, TMR red, Roche) according to the protocol provided by the manufacturer (available online at http://www.roche-applied-science.com).

Immunohistochemistry

Sections were blocked with 3 % hydroxide and 10 % of methyl alcohol for immunoreactivity. Sections were incubated in blocking serum, 10% normal donkey serum in 0.3% triton with PBS. Subsequently, sections were incubated in primary antibody solution for 1 hour at room temperature and overnight at 4℃. To evaluate microglial or astroglial activation and AD-related pathology, primary antibodies including those for mouse anti-

OX-6 (BD bioscience, 1:1000), mouse anti-glial fibrillary acidic protein (GFAP) (BD bioscience, 1:1000), mouse anti-amyloid β 1-42 (Covance, 1:1000), mouse anti-amyloid precursor protein (APP) (Chemicon, 1:2000) and mouse anti-tau-2 (Sigma Aldrich, 1:2000) were used. Sections were washed in PBS with 0.3% Triton X-100 and incubated in a secondary antibody (biotinylated horse anti-mouse antibody, Vector, 1:200) solution for 1 hour at room temperature. Sections were then incubated in extravidin peroxidase solution for one hour at room temperature and visualized with diaminobenzidine solution (Vector SG kit, Vector). Stained sections were mounted on resin-coated slides and dried for a week. Slides were then defatted in xylene and cover-slipped with permount.

To evaluate microglial activation originated from brain, neuronal morphology, and capillary damage, immunofluorescence study was performed, Sections were washed with in PBS with 0.3% Triton X-100 and then incubated in blocking serum, 5% normal donkey serum in 0.15% triton with PBS. Subsequently, sections were incubated in primary antibody solution for 18 hour at room temperature. Mouse anti-OX-6 (BD bioscience, 1:1000), rabbit anti-Iba-1 (Wako, 1:500), mouse anti-NeuN (Chemicon, 1:1000), rabbit anti-MAP-2 (Sigma Aldrich, 1:500) and rabbit anti-laminin (Sigma Aldrich, 1:500) were used, Sections were washed in PBS with 0.15% Triton X-100 and incubated in a secondary antibody solution (Alexa® 568 conjugated donkey anti-rabbit antibody, Alexa® 488 conjugated donkey anti-mouse antibody, 1:200) for 3 hour at room temperature. Stained sections were mounted on resin-coated slides and dried for 30 min. Slides were then cover-slipped with ProLong® Gold antifade reagent (invitrogen).

Quantitative analysis

Sections including the cortex, striatum, hippocampus, and white matter region from four rats per group were subjected to analysis. For a quantitative analysis, we selected specific lesions in which typical cell death or neuroinflammatory changes had been reported in the literature.[6-8]

White matter regions, including those in the corpus callosum, fimbria of the hippocampus, and the internal capsule, were the focus for the quantification of microglial activation. One region of interest (ROI) of $0.5mm^2$ per one section in the corpus callosum (bregma -2.04 to -3.60 mm; 6 sections per rat) and fimbria of the hippocampus (bregma -3.36 to -3.72 mm; 6 sections per rat) were selected. The number of OX-6 microglial cells was counted in each ROI and averaged. To confirm OX-6 positive activated microglial cells were originated from the central nervous system, co-localization study with Iba-1 was performed.

Hippocampal CA1, CA3, and the dentate gyrus were the focus for the quantification of astroglial activation. Five ROIs of $0.01mm^2$ per one section in the CA1, CA3 and dentate gyrus of the hippocampus (bregma -3.24 to -3.72 mm; 6 sections per rat) were selected. The number of GFAP positive astrocytes was counted in each ROI and averaged.

Serial cortical sections were the focus for the quantification of AD-related pathology. Two ROIs of $0.01mm^2$ (APP) and $0.04\ mm^2$ (tau-2) per one cortical section (bregma 2.5 to -1.3mm; 3 sections per rat) were selected. The number of APP or tau-2 positive neurons was counted in each ROI and averaged.

Quantitative analysis of the capillary vascular injury was carried out by modification of the method described in a previous study.[2] The profiles of laminin-positive vascular basement membrane in the cortex were analyzed. Individual length of the fragmentary capillaries in 2 ROIs of $1.5mm^2$ per one cortical section (bregma 2.5 to -1.3mm; 3 sections per rat) was measured using the ImageJ software and summated length was expressed as total capillary length in mm of laminin-positive vascular profiles per mm^3. All quantitative analyses were carried out in a blind manner.

Supplemental References

1. Sasaki H, Inoue T, Iso H, Fukuda Y. Recovery of visual behaviors in adult hamsters with the peripheral nerve graft to the sectioned optic nerve. *Exp Neurol*. 1999;159:377-390.

2. Bell RD, Winkler EA, Sagare AP, Singh I, LaRue B, Deane R, et al. Pericytes control key neurovascular functions and neuronal phenotype in the adult brain and during brain aging. *Neuron*. 2010;68:409-427.

3. Winters BD, Bussey TJ. Transient inactivation of perirhinal cortex disrupts encoding, retrieval, and consolidation of object recognition memory. *J Neurosci*. 2005;25:52-61.

4. Mullani NA, Herbst RS, O'Neil RG, Gould KL, Barron BJ, Abbruzzese JL. Tumor blood flow measured by PET dynamic imaging of first-pass ^{18}F-FDG uptake: a comparison with ^{15}O-labeled water-measured blood flow. *J Nucl Med*. 2008;49:517-523.

5. Nishio K, Ihara M, Yamasaki N, Kalaria RN, Maki T, Fujita Y, et al. A mouse model characterizing features of vascular dementia with hippocampal atrophy. *Stroke*. 2010;41:1278-1284.

6. Liu J, Jin DZ, Xiao L, Zhu XZ. Paeoniflorin attenuates chronic cerebral hypoperfusion-induced learning dysfunction and brain damage in rats. *Brain Res*. 2006;1089:162-170.

7. Whitehead SN, Hachinski VC, Cechetto DF. Interaction between a rat model of cerebral ischemia and beta-amyloid toxicity: inflammatory responses. *Stroke*. 2005;36:107-112.

8. Farkas E, Donka G, de Vos RA, Mihaly A, Bari F, Luiten PG. Experimental cerebral hypoperfusion induces white matter injury and microglial activation in the rat brain. *Acta Neuropathol*. 2004;108:57-64.